

In-depth investigation of the interaction between DNA and nano-sized graphene oxide



Jieon Lee^a, Yeajee Yim^b, Seongchan Kim^b, Myung-Ho Choi^b, Byong-Seok Choi^c, Younghoon Lee^c, Dal-Hee Min^{a,b,d,*}

^a Center for RNA Research, Institute for Basic Science, Seoul National University, Seoul 151-747, Republic of Korea

^b Department of Chemistry, Seoul National University, Seoul 151-747, Republic of Korea

^c Department of Chemistry, Korea Advanced Institute of Science and Technology (KAIST), Daejeon 305-701, Republic of Korea

^d Institute of Nanobio Convergence Technology, Lemonex, Inc., Seoul 151-742, Republic of Korea

ARTICLE INFO

Article history:

Received 15 June 2015

Received in revised form 27 July 2015

Accepted 31 July 2015

Available online 31 August 2015

ABSTRACT

Graphene oxide (GO) has been harnessed in diverse biomedical applications such as drug delivery, biomolecule detection and enzymatic activity assay for a decade. In specific, optical biosensors have been developed based on the preferential binding of single stranded nucleic acid on GO and fluorescence quenching capability of GO. Recently, nano-size GO (NGO), which is smaller than micro-sized large GO (LGO), was employed for live cell imaging of various biomarkers and intracellular RNA. However, in contrast to the expanded applications of size controlled NGO, in-depth study on the interaction between DNA and NGO was not sufficiently carried out. Here, we investigated the DNA length dependent interaction between DNA and NGO. By using three DNA strands having different lengths, we observed (1) kinetics and capacity of DNA adsorption, (2) kinetics and sensitivity of sequence specific desorption of DNA and (3) relative strength of DNA interaction with NGO compared to LGO. Present study will give useful information on the effect of GO size to its interaction with DNA, which are important in developing robust biosensors based on GO and DNA.

© 2015 Published by Elsevier Ltd.

1. Introduction

Graphene is one atom thick 2D carbon nanomaterial with extraordinary electronic, thermal, and mechanical properties [1–3]. Graphene oxide (GO) is a water dispersible derivative of graphene, which has a hexagonal lattice of sp² carbons of graphene and oxygen containing functional groups such as hydroxyl, epoxy, carbonyl and carboxylic acid groups [4]. GO has been recently harnessed in a wide range of applications including electronics [5], electrochemistry [6] and biology [7].

Among the numerous applications of GO, biomedical applications such as drug delivery [8], photothermal therapy [9], cell scaffold [10], biomolecule detection [11–13] and molecular catalysis [14,15] have been under active development for a decade. The newly established systems are aimed to make the impossible assays possible or overcome the disadvantages of conventional analytical methods. For example, GO based helicase enzyme activity assay allowed highly efficient drug candidate screening, which

* Corresponding author at: Center for RNA Research, Institute for Basic Science, Seoul National University, Seoul 151-747, Republic of Korea.

E-mail address: dalheemin@snu.ac.kr (D.-H. Min).

was hardly possible using existing assay methods [16,17]. Common strategy in these applications relies on two properties of GO– (1) strong binding of biomolecules with GO through pi-pi stacking and/or hydrogen bonding interactions and (2) the fluorescence-quenching capability of GO [18,19]. Particularly, preferential binding of single stranded nucleic acid (NA) on GO compared to double stranded NA was the most important principle in the fluorescent NA/GO utilized biosensors [20,21]. The principle has been used to develop NA sensors [12,13], small molecule sensors with aptamer [22,23] and DNA or RNA related enzyme assay platforms [24–26]. More recently, researchers started to extend the GO based systems to analyze biomolecules present in live cells by utilizing nano-sized GO (NGO) [27–29].

Along with the employment of GO for biomolecule sensing platforms, the interaction between ssDNA and GO has been investigated in several reports. For example, DNA adsorption and desorption from GO depending on DNA length [30] and oxidation degree of GO [31], DNA length dependent fluorescence signal in the presence of GO [32] and GO size dependent dynamic range of optical biosensor [33] have been well studied to give useful information in improving the efficiency of general GO based analytical sensors. However, compared with the extensive application of size

controlled NGO, in-depth study for the interaction between DNA and NGO was insufficient. Herein, we investigated the DNA length dependent affinity towards NGO and compared the affinity with micro-sized large GO (LGO) that was generally used in *in vitro* applications. We first studied the kinetics of DNA adsorption on NGO and sequence specific desorption from NGO using three kinds of DNA strands having different number of nucleotides. The NGO based NA adsorption and desorption studies were compared with that of LGO to reveal how the size of GO affects its interaction with DNA. Then, by utilizing deoxyribonuclease I (DNase I), we compared the strength of the DNA-GO interaction according to the size of GO and the length of DNA. It was indirectly judged through the selective digestion of relatively weakly adsorbed DNA on GO (Fig. 1).

2. Experimental

2.1. Materials

Natural graphite (FP 99.95%) was purchased from Graphit Kropfmühl AG (Hauzenberg, Germany). Sulfuric acid (H_2SO_4) was purchased from Samchun chemical (Seoul, Korea). Sodium nitrate ($NaNO_3$) and hydrogen peroxide (30% in water) (H_2O_2) were purchased from Junsei (Japan). Potassium permanganate ($KMnO_4$) and deoxyribonuclease I (DNase I) was purchased from Sigma-Aldrich (MO, USA). Fluorescent dye labelled DNA strands, F-DNA5 (5'-FAM-AGT CA-3'), F-DNA20 (5'-FAM-CTA GCT ATG TGC CTA ATT CA-3') and F-DNA43 (5'-FAM-ATG ATA TCC ATA CAA CTG TCC TTG AAC TTC GGC ACA TAG CTA G-3') were purchased from Genotech (Daejeon, Korea). Unmodified complementary strands, c-DNA5 (5'-TGA CT-3'), c-DNA20 (5'-TGA ATT AGG CAC ATA GCT AG-3') and c-DNA43 (5'-CTA GCT ATG TGC CGA AGT TCA AGG ACA GTT GTA TGG ATA TCA T-3') were also purchased from Genotech (Daejeon, Korea). Fluorescence intensity was measured by using a fluorometer SynergyMax (Biotek, UK).

2.2. Preparation of GO

Crude graphene oxide (CGO) nanosheets were prepared according to previously reported methods [34]. 0.5 g of natural graphite, 0.5 g of $NaNO_3$, and 23 mL of H_2SO_4 were mixed under vigorous stirring in an ice bath. Then, 3 g of $KMnO_4$ was slowly added. After the addition, the mixed solution was transferred to a 35 °C water bath for an hour with stirring. Next, 40 mL of distilled water was added and the bath temperature was increased up to 90 °C for

30 min. Another 100 mL of distilled water was then added. Next, dropwise addition of 3 mL of 30% H_2O_2 changed the color of the solution from dark brown to yellow. The final mixture was filtered through filter paper (Number 3, Whatman) and washed with copious water until the filtrate was neutralized. The filtered solid was dried under reduced pressure for 48 h. Then, LGO sheet was prepared by centrifugation of the CGO suspension (0.1 mg/mL) at 6500 rpm for 30 min. NGO sheet was prepared by subsequent vacuum filtration through 1 μ m and 200 nm pore sized polycarbonate membranes.

2.3. DNA adsorption on GO followed by sequence specific desorption from GO

To prepare DNA/GO complex, 10 μ L of 1 μ M FAM labeled DNA strands was mixed with 0–16 μ L of 0.1 mg/ml GO stock in 90 μ L of pH 7.4 buffer containing 50 mM Tris-HCl and 50 mM NaCl. After 20 min, 10 μ L of 0.5 μ M unmodified target DNA strand was added to the mixture. Fluorescence intensity of each probe was measured at 520 nm.

2.4. DNase I catalyzed DNA digestion adsorbed on GO

To prepare DNA/GO complex, 10 μ L of 1 μ M FAM labeled DNA strand was mixed with 0–16 μ L of 0.1 mg/ml GO stock in 90 μ L of pH 7.4 buffer containing 50 mM Tris-HCl and 50 mM NaCl. After 20 min, 10 μ L of 300 U/ml DNase I was added to the mixture. Fluorescence intensity of each probe was measured at 520 nm.

3. Results and discussion

3.1. Characterization of GO

Before the full-scale investigation of DNA-GO interaction, we prepared two types of GO-NGO and LGO-through size separation of crude GO prepared by using a modified Hummers' method [34]. As-synthesized crude GO (CGO) was composed of carbon sheets with broad size distribution. The LGO and NGO were obtained by centrifugation and physical filtration of CGO using 200 nm pore sized filter. The size of two kinds of single layer GO sheet was observed by atomic force microscopy (AFM) and the height profile. Fig. 2a and b showed AFM images of nanometer sized NGO and micrometer sized LGO sheets. The difference in size was also confirmed by transmission electron microscopy (TEM) images (Fig. S1a). The single layered state was confirmed via the

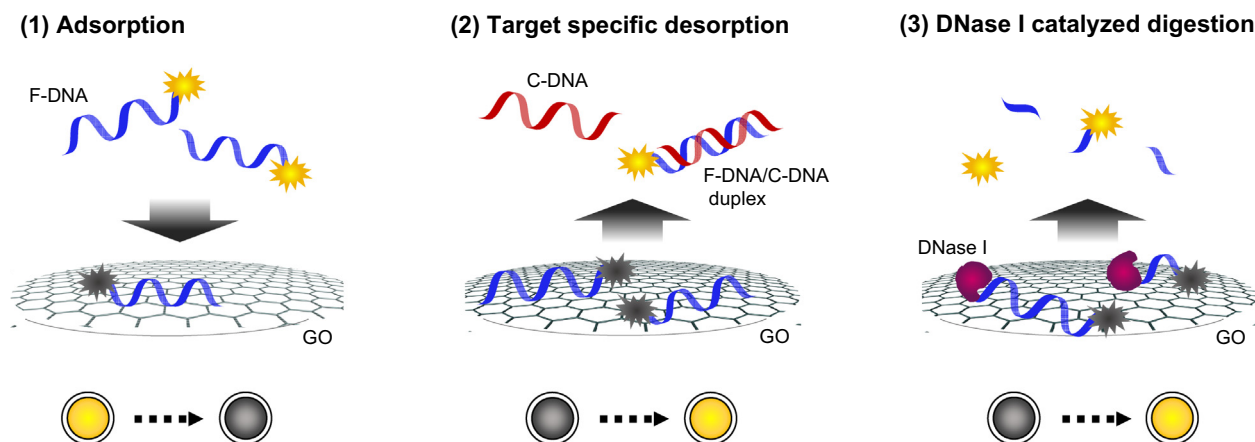


Fig. 1. Investigation of the interaction between DNA and GO through DNA adsorption on GO, sequence specific desorption from GO and DNase I catalyzed DNA digestion. In the present study, three different kinds of fluorescent dye conjugated DNAs having varying lengths and two kinds of GO having different sizes were utilized.

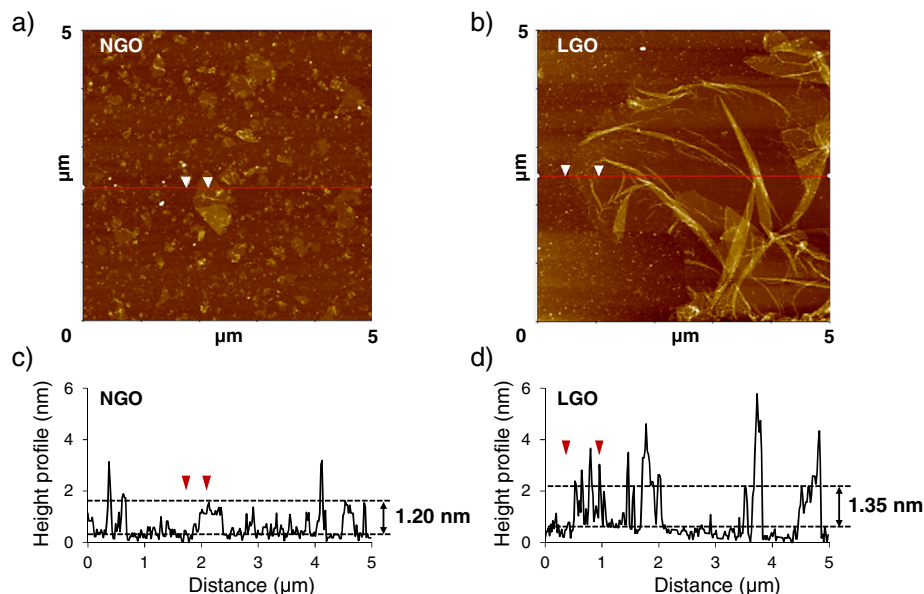


Fig. 2. AFM images and height profile of (a and c) NGO and (b and d) LGO.

height profile showing ca. 1.20 and 1.35 nm thickness of NGO and LGO, respectively (Fig. 2c and d) [35]. The size distribution in aqueous suspension was measured by dynamic light scattering (DLS) analysis based on hydrodynamic radius (HR), resulting in the mean HR around 70 and 3000 nm of NGO and LGO, respectively (Fig. S1a). We further characterized two types of GO by using Raman, UV–Vis absorption, Fourier transform infrared (FT-IR) and X-ray photoelectron spectroscopies. The Raman spectrum showed characteristic peaks at 1352 and 1601 cm^{-1} , respectively assigned as D peak related to structural disorder and G peak from the ordered sp^2 domain (Fig. S1b). The UV–Vis absorption spectrum showed an absorption maxima at 234 nm corresponding to the π – π^* transition of aromatic C=C bonds (Fig. S1c). The peaks in FT-IR spectrum were assigned as oxygen containing functional groups of GO (Fig. S1d). The XPS spectra revealed that the ratio of C–O vs O=C–O was smaller in NGO than LGO, which indicated the degree of oxidation was higher and more carboxyl groups existed in NGO (Fig. S1f) [36]. Collectively, we successfully prepared two different GO, NGO and LGO, which can be categorized as “nano graphene oxide” and “micro graphene oxide” according to previously proposed classification framework [37].

3.2. DNA adsorption on NGO

To investigate the length dependent DNA adsorption on the surface of GO, we chose three types of fluorescein amidite (FAM) labeled DNA oligomers—5, 20 and 43-mer oligonucleotides. F-DNA5 (5'-FAM-AGT CA-3'), F-DNA20 (5'-FAM-CTA GCT ATG TGC CTA ATT CA-3') and F-DNA43 (5'-FAM-ATG ATA TCC ATA CAA CTG TCC TTG AAC TTC GGC ACA TAG CTA G-3') were composed of four different bases possessing the GC content around 40% for comparing the effect of DNA length on the interaction with GO. The degree of F-DNA adsorption on GO could be indirectly observed by measuring the fluorescence intensity of the dye conjugated to DNA as reported previously.

3.2.1. DNA adsorption capacity of NGO

We performed DNA length dependent adsorption test using NGO as well as LGO. F-DNA strands with three different length were prepared in pH 7.4 buffered solutions containing metal cations (20 mM Tris-HCl, 2.5 mM MgCl_2 , and 0.5 mM CaCl_2) for

facilitating poly-anionic DNA adsorption on negatively charged GO. Upon incubation of DNA and GO in the buffered solution for 20 min, the fluorescence intensity of F-DNA decreased depending on the concentration of NGO and LGO, regardless of the length of F-DNA. However, the amount of GO required for notable fluorescence quenching of F-DNA was varied depending on the length of F-DNA. In case of NGO, the fluorescence intensity of shortest F-DNA, F-DNA5, declined most dramatically depending on the concentration of GO, whereas longer F-DNAs showed gradual decrease of fluorescence intensity (Fig. S2a). As a result, each fluorescence intensity of 100 nM of F-DNA5, 20 and 43 was quenched down to ~5% upon addition of 1, 2 and 4 $\mu\text{g}/\text{ml}$ of NGO, respectively (Fig. 3a). The tendency of DNA length dependent adsorption capacity was also observed in LGO (Fig. S2b, Fig. 3b). This result well agrees with previous studies performed with CGO showing that shorter DNA was more efficiently adsorbed on GO [30]. It indicated that the size of GO hardly gave significant effect on the loading capacity of DNA strands on its surface.

3.2.2. DNA adsorption kinetics on NGO

In order to further investigate the adsorption of DNA on GO, we performed adsorption kinetics by measuring the fluorescence intensity of F-DNA in the presence of GO over time. In the above mentioned GO-containing buffered solution, the decline of the fluorescence intensity of all three F-DNAs reached to equilibrium within 20 min. In both cases of NGO and LGO, longer DNA showed slower decrease of fluorescence intensity, which is consistent with previous reports performed using CGO containing various sizes of GO [30]. Kinetic data suggested that NGO, smaller sized GO, promoted faster adsorption compared to LGO. This phenomenon could be probably explained by the difference in diffusion rate between NGO and LGO. Taken together, DNA adsorption could be achieved more quickly if shorter DNA and smaller GO was utilized (Fig. 4).

3.3. Sequence specific desorption of DNA from NGO

Next, we compared the efficiency of sequence specific F-DNA desorption from NGO by adding complementary target c-DNA to the pre-complexed DNA/NGO. Unmodified strands, c-DNA5 (5'-TGA CT-3'), c-DNA20 (5'-TGA ATT AGG CAC ATA GCT AG-3') and c-DNA43 (5'-CTA GCT ATG TGC CGA AGT TCA AGG ACA GTT GTA

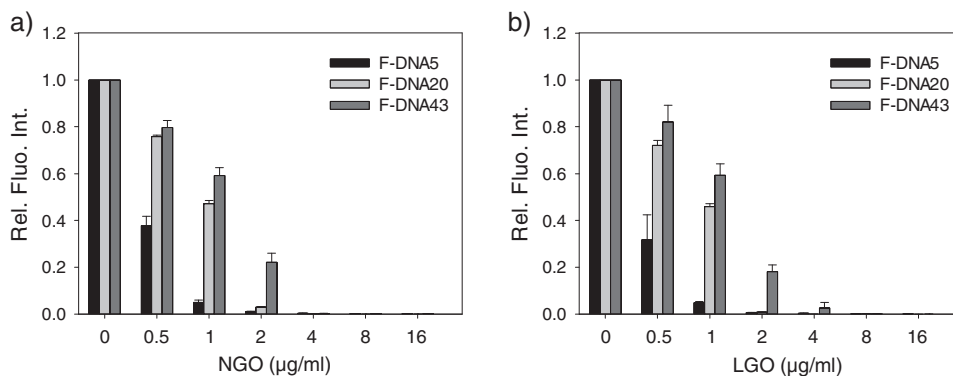


Fig. 3. DNA length-dependent adsorption on two types of GO. Relative fluorescence intensity of three kinds of F-DNA in the presence of various concentrations of (a) NGO and (b) LGO.

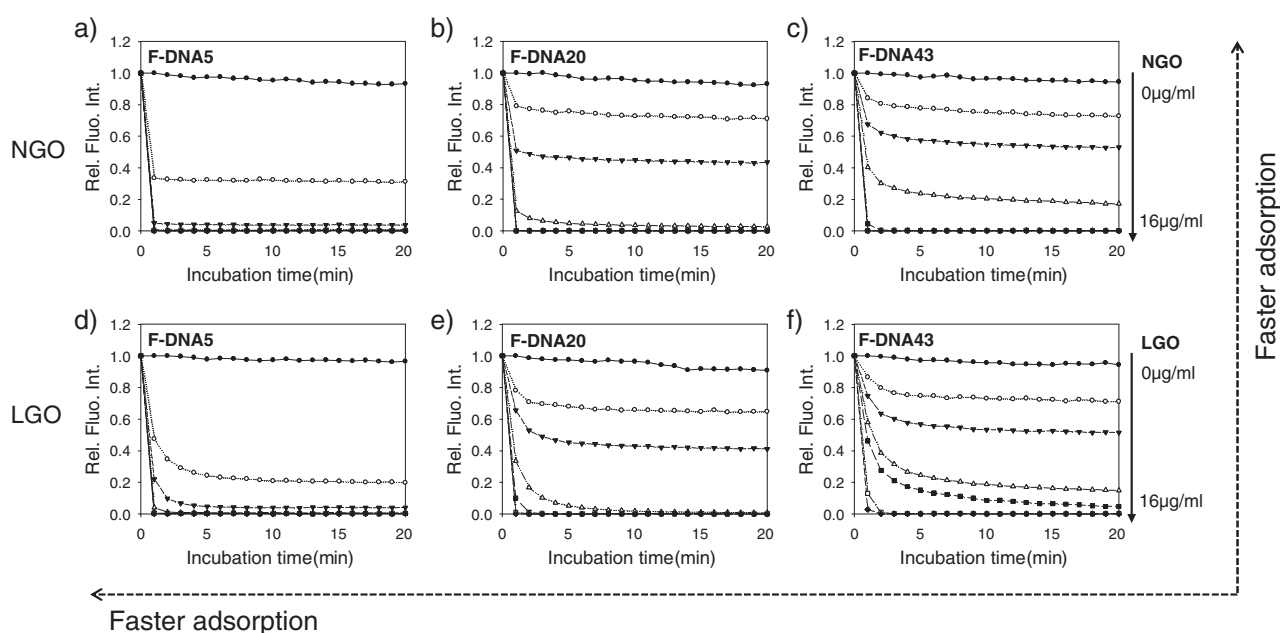


Fig. 4. Adsorption kinetics of three kinds of F-DNA having different length to GO surface at various concentrations of (a, b and c) NGO and (d, e and f) LGO.

TGG ATA TCA T-3'), were utilized as fully complementary sequences of DNA to F-DNA5, 20, 43, respectively. 100 nM of each F-DNA was pre-incubated with various concentrations of NGO for 20 min to build the F-DNA/NGO complex and then, 5 pmol of each corresponding target was added to the mixture (Fig. S3a). As a control, the sequence specific desorption test was repeated using LGO in place of NGO (Fig. S3b). The shortest strand, F-DNA5, showed little increase of intensity in both cases of NGO and LGO due to the low melting temperature (T_m) between the two DNA strands than room temperature [38]. F-DNA20 and F-DNA43 showed remarkable fluorescence recovery at each optimal GO concentration, 2 and 4 $\mu\text{g/ml}$, regardless of the size of GO, respectively (Fig. 5).

The optimal concentrations of GO for each sequence specific desorption were identical with the minimum amount of GO required for maximum quenching of the fluorescence of corresponding F-DNA. At GO concentration lower than the optimum value, there was higher chance of the hybridization between target c-DNA and free F-DNA that is not adsorbed onto GO. On the other hand, at higher GO concentration, it was easier for free single stranded target c-DNA to interact with excess GO rather than forming c-DNA/F-DNA duplex. The sequence specific desorption kinetics of them, in contrast with adsorption kinetics, represented

similar fluorescence increase, regardless of DNA length and GO size (Fig. S4). Lastly, we calculated the percentage of recovered intensity using relative fluorescence intensity of F-DNA only, F-DNA/GO, and F-DNA/GO/target c-DNA under the optimized experimental condition. Each percentage of recovered intensity ($=100 \times (F_{\text{F-DNA/GO/target}}/F_{\text{F-DNA only}} - F_{\text{F-DNA/GO}}/F_{\text{F-DNA only}})$), shown on the top of the bar graph, was considered as a ratio of detached F-DNA from GO by hybridization with complementary c-DNA strand. As a result, except for the shortest strand possessing lower T_m value than room temperature, 38% of F-DNA20 and 16% of F-DNA43 was desorbed from NGO through hybridization with complementary strand (Fig. 6a). The desorption efficiency of NGO was slightly higher than LGO, under the experimental condition (Fig. 6a and b). The result could be partially due to the higher proportion of carboxyl groups in NGO, which provides an additional driving force to detach the F-DNA from GO surface in the presence of target nucleic acid, compared to LGO [33].

3.4. Interaction strength between DNA and GO

We next performed an experiment to compare the strength of interaction between DNA and GO by using DNase I. DNase I is a

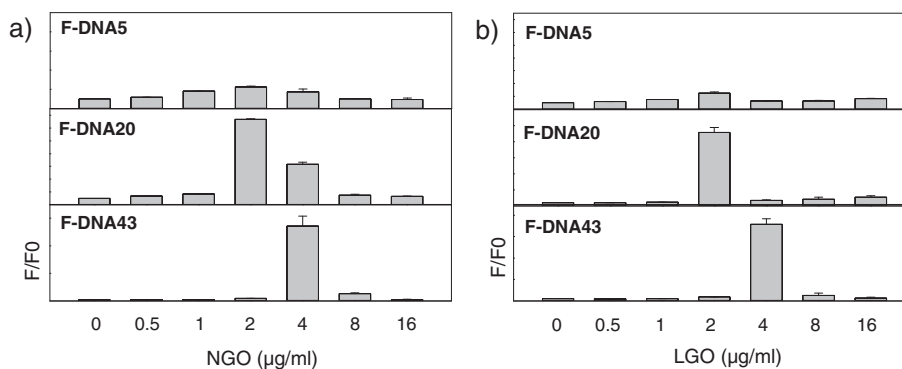


Fig. 5. F/F0 values of F-DNA/GO complex in the presence of each complementary target (50 nM). Each F-DNA was pre-incubated with various concentrations of (a) NGO and (b) LGO.

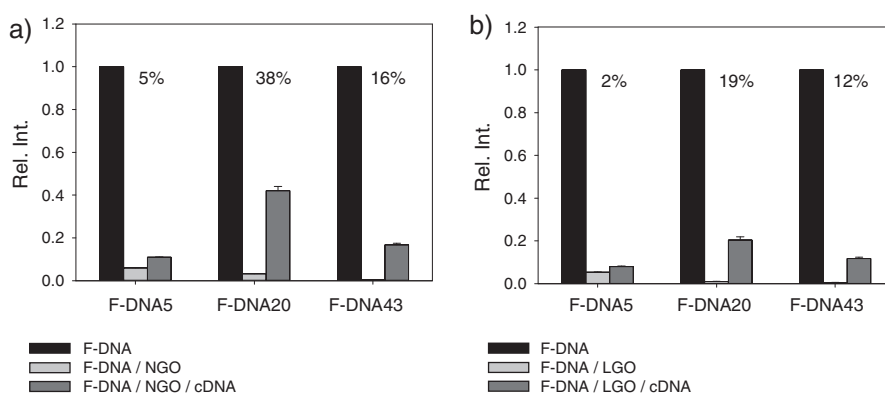


Fig. 6. Relative fluorescence intensity of F-DNA in the presence of GO and target DNA. (a) Each F-DNA with three different length was adsorbed on GO ((a) NGO, (b) LGO) of which amount was determined for quenching the fluorescence of F-DNA up to 95%. 1, 2 and 4 µg/ml GO were utilized for adsorption and fluorescence quenching of 5, 20 and 43 mer F-DNA, respectively. Relative fluorescence recovery percentages ($=100 \times (F_{\text{F-DNA/GO/target}}/F_{\text{F-DNA only}} - F_{\text{F-DNA/GO}}/F_{\text{F-DNA only}})$) were shown on top of the bar graph. To test the efficiency of sequence specific desorption of F-DNA from GO, 50 nM of each target c-DNA was added to the corresponding DNA/GO complex.

deoxyribonuclease which hydrolyzes the DNA nonspecifically to release di-, tri- and oligonucleotide products [39]. In a lot of previous reports, DNase I has been employed in GO based nucleic acid sensing system as a signal amplifier [40,41]. The strategy for signal amplification was based on inaccessibility of DNase I to adsorbed DNA on GO or in other words, selective digestion of desorbed DNA from GO or loosely bound DNA to GO by DNase I. In fact, the experimental condition of DNase I in sensing system was well-established to maximize the selectivity of DNase I activity for digestion of desorbed DNA specifically. Upon the application of excess amount of DNase I on DNA/GO system, it also affected on DNA strands even adsorbed on GO [42], resulting in cleavage of weakly adsorbed DNA on GO. Thus, we utilized DNase I to correlate the interaction strength between DNA and GO according to the length of DNA and the size of GO. The excess DNase I also enabled to stabilize the recovered signal by breaking up desorbed DNA strands to short nucleotides, of which fluorescence could not be quenched by GO.

3.4.1. DNase I catalyzed digestion of DNA on GO

In order to re-confirm the DNase I activity against DNA strands in the presence of GO, we measured the fluorescence intensity of F-DNA5/LGO complex after addition of DNase I. As a control, inactivated DNase I was prepared by heating the enzyme stock at 75 °C for 20 min. F-DNA5 was pre-incubated with LGO in a buffered solution for 20 min to build the DNA/GO complex. Then, active DNase I and inactivated DNase I were added to F-DNA/GO complex. As expected, addition of active DNase I to F-DNA/GO resulted in

remarkable fluorescence recovery depending on concentration of DNase I, whereas inactivated DNase I had little effect on the fluorescence intensity of F-DNA/GO complex. This data supported that DNase I mediated increase of the fluorescence signal was induced by digestion of DNA rather than the nonspecific desorption of F-DNA from GO by DNase I-GO interaction (Fig. S5).

3.4.2. Investigation of the interaction between DNA and GO using DNase I

For the DNase I catalyzed digestion of DNA adsorbed on GO, three different DNA strands were first incubated with each optimal GO concentration in buffered condition to induce adsorption of sufficient amount of DNA strands on GO with more than 95% of fluorescence quenching. When 100 nM of F-DNA5, 20 and 43 was added to 1, 2 and 4 µg/ml of NGO and LGO, respectively, the fluorescence signal of F-DNA was quenched up to 95% in 20 min. Next, 3 U of DNase I, which was excess amount enough to digest the free corresponding DNA strands in a few minutes, was added to F-DNA/GO complex. After 2 h incubation, the F-DNA5/NGO showed fluorescence increase up to more than 50% of initial intensity of free F-DNA5, whereas the recovered intensities of F-DNA20/NGO and F-DNA43/NGO reached to only 27% and 12% of each initial intensities, respectively. In case of LGO, the tendency of DNA length dependent fluorescence recovery was identical with NGO. The percentage of recovered fluorescence intensities reflected the amount of F-DNA digested by DNase I. Thus, this result suggested that shorter DNA possessing fewer bases to interact with the GO surface has weaker affinity against GO and the strength of interaction with

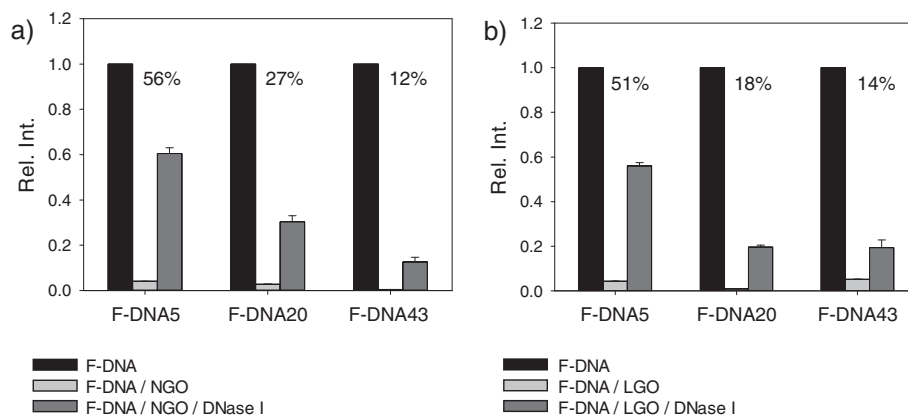


Fig. 7. Relative fluorescence intensity of F-DNA in the presence of GO and DNase. (a) Each F-DNA with three different length was adsorbed on GO ((a) NGO, (b) LGO) of which amount was determined for quenching the fluorescence of F-DNA up to 95%. Each optimally adjusted concentration of GO (1, 2 and 4 $\mu\text{g}/\text{ml}$) was used for adsorption and fluorescence quenching of 5, 20 and 43 mer F-DNA. Relative fluorescence recovery percentages ($=100 \times (F_{\text{F-DNA/GO}/\text{target}}/F_{\text{F-DNA only}} - F_{\text{F-DNA/GO}}/F_{\text{F-DNA only}})$) were shown on top of the bar graph. To test the interaction between DNA and GO, 3 U of DNase I was applied to the F-DNA/GO complex.

DNA is nearly impervious to the size of GO (Fig. 7). In addition, if the fluorescence recovery was calculated to F/F_0 value, the histogram versus GO concentration was broader than that of sequence specific desorption, and the maximum F/F_0 of that was not observed at each optimal GO concentration. Considering the interruption of fluorescence increase induced by the preferential digestion of free DNA by DNase I in the range of low GO concentrations [40,41] and enzyme activity inhibition in the range of high GO concentrations [43], DNA digestion in the presence of GO by DNase I would not be highly dependent on the amount of GO under the experimental condition. The result suggests that the interaction between adsorbed DNA and GO is not likely to be notably affected by total amount of GO (Fig. S6).

4. Conclusion

In summary, we investigated the length dependent interaction of DNA with NGO and compared the result with the case of LGO. By using three different DNAs having varying lengths, we measured the DNA adsorption capacity and kinetics against two differently sized GOs. We found that (1) shorter DNA was more effectively loaded on GO regardless of GO size and (2) shorter DNA showed faster adsorption kinetics with smaller GO (NGO). Next, the experiments on desorption of DNA from NGO was performed using each complementary c-DNA. Upon addition of corresponding target c-DNA in various F-DNA/NGO complex, fluorescence recovery efficiency was highest at minimal amount of NGO which quenched the fluorescence intensity of F-DNA down to $\sim 5\%$. Desorption from LGO followed the trend of NGO, but the F/F_0 value was lower than that of NGO. Lastly, for demonstrating the strength of interaction between DNA and GO, DNase I was utilized for digestion of weakly adsorbed DNA on GO. Upon addition of DNase I to F-DNA adsorbed on GO, shortest F-DNA showed highest fluorescence recovery in both cases of NGO and LGO, suggesting that shorter F-DNA might be bound on GO less tightly or its association and dissociation with GO is faster compared to longer F-DNA. Also, broad histogram of F/F_0 value versus GO concentration indicates that the interaction between DNA and GO is not sensitive to the amount of GO. We believe that the present study will provide useful basic information in the development of more efficient and practically useful DNA/GO based sensors in the future.

Acknowledgments

This work was supported by the Basic Science Research Program (2011-0017356, 2011-0020322), International S&T

Cooperation Program (2014K1B1A1073716) and the Research Center Program (IBS-R008-D1) of IBS (Institute for Basic Science) through the National Research Foundation of Korea (NRF) and Research Program (C0193918) through the SMBA funded by the Korean government (MEST).

Appendix A. Supplementary data

Supplementary data associated with this article can be found, in the online version, at <http://dx.doi.org/10.1016/j.carbon.2015.07.093>.

References

- [1] K.S. Novoselov, A.K. Geim, S.V. Morozov, D. Jiang, Y. Zhang, S.V. Dubonos, et al., Electric field effect in atomically thin carbon films, *Science* 306 (5696) (2004) 666–669.
- [2] M.J. Allen, V.C. Tung, R.B. Kaner, Honeycomb carbon: a review of graphene, *Chem. Rev.* 110 (1) (2010) 132–145.
- [3] F. Kim, L.J. Cote, J. Huang, Graphene oxide: surface activity and two-dimensional assembly, *Adv. Mater.* 22 (17) (2010) 1954–1958.
- [4] Y. Zhu, S. Murali, W. Cai, X. Li, J.W. Suk, J.R. Potts, et al., Graphene and graphene oxide: synthesis, properties, and applications, *Adv. Mater.* 22 (35) (2010) 3906–3924.
- [5] G. Eda, M. Chhowalla, Chemically derived graphene oxide: towards large-area thin-film electronics and optoelectronics, *Adv. Mater.* 22 (22) (2010) 2392–2415.
- [6] M. Pumera, Electrochemistry of graphene, graphene oxide and other graphenoids: review, *Electrochem. Commun.* 36 (2013) 14–18.
- [7] C. Chung, Y.K. Kim, D. Shin, S.R. Ryoo, B.H. Hong, D.H. Min, Biomedical applications of graphene and graphene oxide, *Acc. Chem. Res.* 46 (10) (2013) 2211–2224.
- [8] Z. Liu, J.T. Robinson, X.M. Sun, H.J. Dai, PEGylated nanographene oxide for delivery of water-insoluble cancer drugs, *J. Am. Chem. Soc.* 130 (33) (2008) 10876–10877.
- [9] M. Li, X. Yang, J. Ren, K. Qu, X. Qu, Using graphene oxide high near-infrared absorbance for photothermal treatment of Alzheimer's disease, *Adv. Mater.* 24 (13) (2012) 1722–1728.
- [10] W. Li, J. Wang, J. Ren, X. Qu, 3D graphene oxide-polymer hydrogel: near-infrared light-triggered active scaffold for reversible cell capture and on-demand release, *Adv. Mater.* 25 (46) (2013) 6737–6743.
- [11] L. Wu, X. Qu, Cancer biomarker detection: recent achievements and challenges, *Chem. Soc. Rev.* 44 (10) (2015) 2963–2997.
- [12] C.H. Lu, H.H. Yang, C.L. Zhu, X. Chen, G.N. Chen, A graphene platform for sensing biomolecules, *Angew. Chem. Int. Edit.* 48 (26) (2009) 4785–4787.
- [13] J. Lee, I.S. Park, E. Jung, Y. Lee, D.H. Min, Direct, sequence-specific detection of dsDNA based on peptide nucleic acid and graphene oxide without requiring denaturation, *Biosens. Bioelectron.* 62 (2014) 140–144.
- [14] Y. Liu, D.S. Yu, C. Zeng, Z.C. Miao, L.M. Dai, Biocompatible graphene oxide-based glucose biosensors, *Langmuir* 26 (9) (2010) 6158–6160.
- [15] Y.J. Song, K.G. Qu, C. Zhao, J.S. Ren, X.G. Qu, Graphene oxide: intrinsic peroxidase catalytic activity and its application to glucose detection, *Adv. Mater.* 22 (19) (2010) 2206.
- [16] H. Jang, S.R. Ryoo, Y.K. Kim, S. Yoon, H. Kim, S.W. Han, et al., Discovery of hepatitis C virus NS3 helicase inhibitors by a multiplexed, high-throughput

- helicase activity assay based on graphene oxide, *Angew. Chem. Int. Edit.* 52 (8) (2013) 2340–2344.
- [17] H. Jang, S.R. Ryoo, M.J. Lee, S.W. Han, D.H. Min, A new helicase assay based on graphene oxide for anti-viral drug development, *Mol. Cells* 35 (4) (2013) 269–273.
- [18] R.S. Swathi, K.L. Sebastian, Resonance energy transfer from a dye molecule to graphene, *J. Chem. Phys.* 129 (5) (2008).
- [19] R.S. Swathi, K.L. Sebastian, Long range resonance energy transfer from a dye molecule to graphene has (distance)⁻⁴ dependence, *J. Chem. Phys.* 130 (8) (2009).
- [20] S.J. He, B. Song, D. Li, C.F. Zhu, W.P. Qi, Y.Q. Wen, et al., A graphene nanoprobe for rapid, sensitive, and multicolor fluorescent DNA analysis, *Adv. Funct. Mater.* 20 (3) (2010) 453–459.
- [21] B.W. Liu, Z.Y. Sun, X. Zhang, J.W. Liu, Mechanisms of DNA sensing on graphene oxide, *Anal. Chem.* 85 (16) (2013) 7987–7993.
- [22] Y. He, Z.G. Wang, H.W. Tang, D.W. Pang, Low background signal platform for the detection of ATP: when a molecular aptamer beacon meets graphene oxide, *Biosens. Bioelectron.* 29 (1) (2011) 76–81.
- [23] M. Li, X.J. Zhou, W.Q. Ding, S.W. Guo, N.Q. Wu, Fluorescent aptamer-functionalized graphene oxide biosensor for label-free detection of mercury (II), *Biosens. Bioelectron.* 41 (2013) 889–893.
- [24] H. Jang, Y.K. Kim, H.M. Kwon, W.S. Yeo, D.E. Kim, D.H. Min, A graphene-based platform for the assay by helicase, *Angew. Chem. Int. Edit.* 49 (33) (2010) 5703–5707.
- [25] J. Lee, Y.K. Kim, D.H. Min, Laser desorption/ionization mass spectrometric assay for phospholipase activity based on graphene oxide/carbon nanotube double-layer films, *J. Am. Chem. Soc.* 132 (42) (2010) 14714–14717.
- [26] J. Lee, Y.K. Kim, D.H. Min, A new assay for endonuclease/methyltransferase activities based on graphene oxide, *Anal. Chem.* 83 (23) (2011) 8906–8912.
- [27] Y. Wang, Z.H. Li, D.H. Hu, C.T. Lin, J.H. Li, Y.H. Lin, Aptamer/graphene oxide nanocomplex for in situ molecular probing in living cells, *J. Am. Chem. Soc.* 132 (27) (2010) 9274–9276.
- [28] S. Kim, S.R. Ryoo, H.K. Na, Y.K. Kim, B.S. Choi, Y. Lee, et al., Deoxyribozyme-loaded nano-graphene oxide for simultaneous sensing and silencing of the hepatitis C virus gene in liver cells, *Chem. Commun.* 49 (74) (2013) 8241–8243.
- [29] S.R. Ryoo, J. Lee, J. Yeo, H.K. Na, Y.K. Kim, H. Jang, et al., Quantitative and multiplexed microRNA sensing in living cells based on peptide nucleic acid and nano graphene oxide (PANGO), *ACS Nano* 7 (7) (2013) 5882–5891.
- [30] M. Wu, R. Kempaiah, P.J.J. Huang, V. Maheshwari, J.W. Liu, Adsorption and desorption of DNA on graphene oxide studied by fluorescently labeled oligonucleotides, *Langmuir* 27 (6) (2011) 2731–2738.
- [31] B.J. Hong, Z. An, O.C. Compton, S.T. Nguyen, Tunable biomolecular interaction and fluorescence quenching ability of graphene oxide: application to “turn-on” DNA sensing in biological media, *Small* 8 (16) (2012) 2469–2476.
- [32] P.J.J. Huang, J.W. Liu, DNA-length-dependent fluorescence signaling on graphene oxide surface, *Small* 8 (7) (2012) 977–983.
- [33] H. Zhang, S.S. Jia, M. Lv, J.Y. Shi, X.L. Zuo, S. Su, et al., Size-dependent programming of the dynamic range of graphene oxide-DNA interaction-based ion sensors, *Anal. Chem.* 86 (8) (2014) 4047–4051.
- [34] J.Y. Luo, L.J. Cote, V.C. Tung, A.T.L. Tan, P.E. Goins, J.S. Wu, et al., Graphene oxide nanocolloids, *J. Am. Chem. Soc.* 132 (50) (2010) 17667–17669.
- [35] Y.K. Kim, D.H. Min, The structural influence of graphene oxide on its fragmentation during laser desorption/ionization mass spectrometry for efficient small-molecule analysis, *Chem. Eur. J.* 21 (19) (2015) 7217–7223.
- [36] H. Zhang, C. Peng, J. Yang, M. Lv, R. Liu, D. He, Q. Huang, Uniform ultrasmall graphene oxide nanosheets with low cytotoxicity and high cellular uptake, *ACS Appl. Mater. Interfaces* 5 (5) (2013) 1761–1767.
- [37] P. Wick, A.E. Louw-Gaume, M. Kucki, H.F. Krug, K. Kostarelos, B. Fadeel, et al., Classification framework for graphene-based materials, *Angew. Chem. Int. Edit.* 53 (30) (2014) 7714–7718.
- [38] P.M. Howley, M.A. Israel, M.F. Law, M.A. Martin, Rapid method for detecting and mapping homology between heterologous DNAs – evaluation of polyomavirus genomes, *J. Biol. Chem.* 254 (11) (1979) 4876–4883.
- [39] D. Suck, C. Oefner, W. Kabsch, 3-dimensional structure of bovine pancreatic DNase-I at 2.5 Å resolution, *EMBO J.* 3 (10) (1984) 2423–2430.
- [40] Z.W. Tang, H. Wu, J.R. Cort, G.W. Buchko, Y.Y. Zhang, Y.Y. Shao, et al., Constraint of DNA on functionalized graphene improves its biostability and specificity, *Small* 6 (11) (2010) 1205–1209.
- [41] L. Cui, X.Y. Lin, N.H. Lin, Y.L. Song, Z. Zhu, X. Chen, et al., Graphene oxide-protected DNA probes for multiplex microRNA analysis in complex biological samples based on a cyclic enzymatic amplification method, *Chem. Commun.* 48 (2) (2012) 194–196.
- [42] J. Gang, Graphene oxide-based direct measurement of DNase I activity with single stranded DNA, *B. Korean Chem. Soc.* 35 (9) (2014) 2749–2752.
- [43] M. De, S.S. Chou, V.P. Dravid, Graphene oxide as an enzyme inhibitor: modulation of activity of alpha-chymotrypsin, *J. Am. Chem. Soc.* 133 (44) (2011) 17524–17527.